No Chance to Survive: *Mo*-CBP$_3$-PepII Synthetic Peptide acts on *Cryptococcus neoformans* by multiple mechanisms of action

Tawanny K.B. Aguiar[1]; Felipe P. Mesquita[2]; Nilton A.S. Neto[1]; Francisco Í. R. Gomes[1]; Cleverson D. T. Freitas[1]; Rômulo F. Carneiro[3], Celso S. Nagano[3], Luciana M. R. Alencar[4]; Ralph Santos-Oliveira[5,6], Jose T. A. Oliveira[1], Pedro F.N. Souza[1,2*]

[1]Department of Biochemistry and Molecular Biology, Federal University of Ceará, Fortaleza 60451-970, CE, Brazil;

[2]Drug Research and Development Center, Department of Physiology and Pharmacology, Federal University of Ceará, Fortaleza 60430-275, CE, Brazil

[3]Department of Fisheries Engineering, Federal University of Ceará (UFC), Fortaleza, Brazil;

[4]Laboratory of Biophysics and Nanosystems, Physics Department, Federal University of Maranhão,

Maranhão 65080805, Brazil

[5]Brazilian Nuclear Energy Commission, Nuclear Engineering Institute, Rio de Janeiro 21941906, Brazil

[6]Laboratory of Nanoradiopharmacy, Rio de Janeiro State University, Rio de Janeiro 23070200, Brazil

***Correspondence:** Pedro F. N. Souza (pedrofilhobio@gmail.com and pedrofilhobio@ufc.br) at Drug Research and Development Center, Department of Physiology and Pharmacology, Federal University of Ceará, Brazil.

ORCID: 0000-0003-2524-4434 (Pedro F. N. Souza)

ORCID: 0000-0002-7100-0927 (Tawanny K. B. Aguiar)

doi:10.20944/preprints202301.0373.v1

Abstract

Cryptococcus neoformans is a human multidrug-resistant yeast with high mortality rates in immunocompromised patients. Recently, the synthetic peptide *Mo*-CBP$_3$-PepII emerged as a potent anticryptococcal molecule with an MIC50 at low concentration. Here, the mechanisms of action of *Mo*-CBP$_3$-PepII were deeply analyzed to provide new information about how it led *C. neoformans* cells to death. Light and fluorescence microscopies, analysis of enzymatic activities, and proteomic analysis were employed to understand the effect of *Mo*-CBP$_3$-PepII on *C. neoformans* cells. Light and fluorescence microscopies revealed *Mo*-CBP$_3$-PepII induced the accumulation of anion superoxide and hydrogen peroxide in *C. neoformans* cells. In addition to a reduction in the activity of superoxide dismutase (SOD), ascorbate peroxidase (APX), and catalase (CAT) in the cells treated with *Mo*-CBP$_3$-PepII. In the presence of Ascorbic acid (AsA), no ROS were detected and *Mo*-CBP$_3$-PepII lost the inhibitory activity against *C. neoformans*. Yet, *Mo*-CBP$_3$-PepII inhibited the activity of lactate dehydrogenase (LDH), ergosterol biosynthesis, and induced the decoupling of cytochrome *c* from the mitochondrial membrane. Proteomic analysis revealed a reduction in the abundance of proteins related to energetic metabolism, DNA and RNA metabolism, pathogenicity, protein metabolism, cytoskeleton, and cell wall organization and division. Our findings indicated that *Mo*-CBP$_3$-PepII might have multiple mechanisms of action against *C. neoformans* cells, mitigating the development of resistance and thus being a potent molecule to be employed in the production of new drugs against *C. neoformans* infections.

Keywords: alternative drugs, cryptococcosis, oxidative stress, synthetic peptides

1. Introduction

Two decades have passed since the last new antifungal drug was released; however, the incidence of invasive infections by multidrug-resistant Fungi has increased [1]. Three main antifungal classes are available to treat fungal infections: azoles, polyenes, and echinocandins. Nonetheless, their use includes limitations, such as the spectrum of activity, resistance, toxicity, drug-drug interactions, and poor bioavailability [2].

In a list of priority regarding fungal pathogens recently published by the World Health Organization (WHO) [3], *Cryptococcus neoformans* appears in the top three due to some reasons: (1) low susceptibility to current antifungal agents; (2) poorly understood resistance to drugs; and (3) high mortality rate ranging from 41% to 61% [3]. *C. neoformans* causes cryptococcosis, which mainly occurs in the lungs and leads to pneumonia but also affects the brain, causing meningitis, mostly in patients with a compromised immune system [3,4]. HIV^+ patients, individuals with cancer, or taking any drug that weaken the immune system are predisposed to acquire cerebral cryptococcosis, which forms lesions known as cryptococcomas [3]. *C. neoformans* is naturally resistant to azole antifungals and the latest antifungal drug, Caspofungin, causing global health concerns [5,6]. Therefore, the search for new alternatives to treat cryptococcosis becomes emerging. In this context, antimicrobial peptides (AMPs) appear as a promise due to their mechanisms of action on the membrane [7].

Natural AMPs have limitations in their use and are generally cytotoxic. Moreover, the rational design of synthetic antimicrobial peptides (SAMPs) is an alternative to this problem. This approach is cost-effective for active short peptides [7–9]. Recently, our research group assessed the anticryptococcal potential of *Mo*-CBP$_3$-PepII [10], a synthetic peptide bioinspired in the sequence of *Mo*-CBP$_3$, a protein purified from *Moringa oleifera* seeds [11]. This study demonstrated that *Mo*-CBP$_3$-PepII has an MIC50 of 25 μg mL^{-1} and induced membrane pore formation, DNA degradation, and apoptosis

doi:10.20944/preprints202301.0373.v1

in cryptococcal cells. Additionally, it was reported that *Mo*-CBP$_3$-PepII interacts with ergosterol in the membrane of *C. neoformans* favoring pore formation [10].

Here, new insights were provided about the mechanisms of action employed by *Mo*-CBP$_3$-PepII against *C. neoformans*. Our analysis revealed that *Mo*-CBP$_3$-PepII stimulates oxidative stress, inhibits ergosterol biosynthesis, and induces the decoupling of cytochrome *c* from mitochondria. In addition, *Mo*-CBP$_3$-PepII promotes changes in the proteomic profile of *C. neoformans*.

2. Results and Discussion

2.1. *Mo*-CBP$_3$-PepII induced ROS overaccumulation in C. neoformans cells

All experiments in this study were carried out using the MIC50 concentration of 25 µg mL^{-1} of *Mo*-CBP$_3$-PepII against *C. neoformans* as defined in our previous published study by Aguiar et al. [10]. The *Mo*-CBP$_3$-PepII-treated *C. neoformans* cells showed an accumulation of reactive oxygen species (ROS) anion superoxide ($O2^{\bullet-}$) and hydrogen peroxide (H_2O_2) (Fig. 1). The light microscopy analysis revealed the accumulation of $O2^{\bullet-}$ in *Mo*-CBP$_3$-PepII-treated *C. neoformans* cells (Fig. 1 - blue or cyan dots – black arrows). As expected, the same was not observed in control cells (DMSO-NaCl) (Fig. 1). The detection of H_2O_2 was carried out by fluorescence microscopy using 2′,7′ dichlorofluorescein diacetate (DCFH-DA, Sigma, St. Louis, MI, 364 USA) assay. The green fluorescence on cells indicates the accumulation of H_2O_2 after treatment with *Mo*-CBP$_3$-PepII. In contrast, DMSO-NaCl not showed the same (Fig. 1 - H_2O_2 panel).

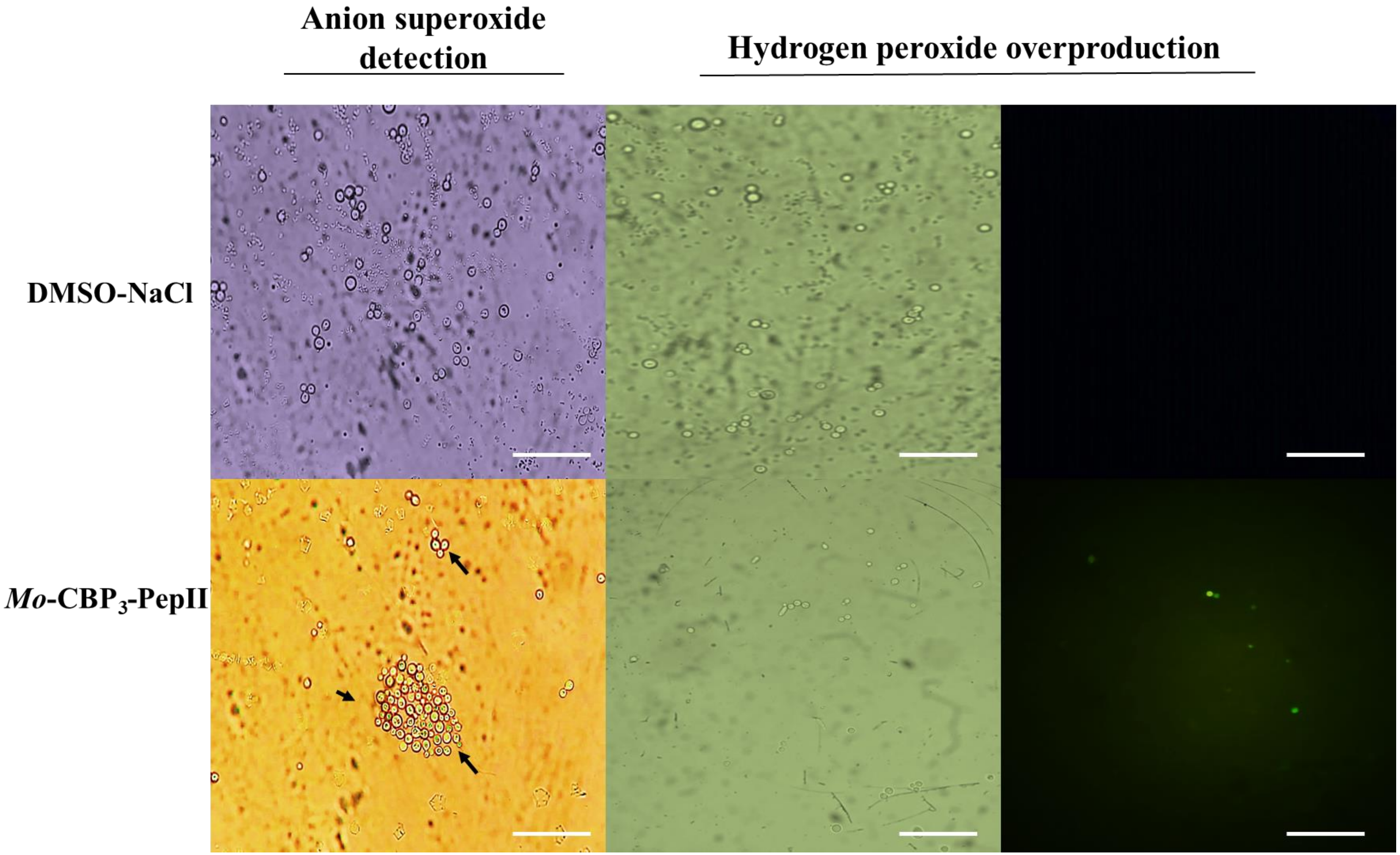

Figure 1. Detection of anion superoxide and hydrogen peroxide in *C. neoformans* cells. Light and fluorescence microscopies analysis to detect, respectively, the conversion of NBT into formazan (blue or cyan dots – black arrows) and the accumulation of hydrogen peroxide in *C. neoformans* cells treated with *Mo*-CBP$_3$-PepII at MIC50 concentration. White bars indicate 100 µm.

ROS are inherent molecules of life as a byproduct of aerobic cell metabolism, and it is impossible to leave without them. Besides, ROS plays several essential roles in cell life, growth, development, defense, and signaling [12]. For pathogens such as Fungi, ROS play critical roles in biofilm biogenesis, infection, virulence, and developmental process [13]. Even though these are good effects of ROS, the induction of ROS overproduction is a mechanism of action employed by antimicrobial peptides to kill human pathogenic Fungi [7,14–17]. What is essential to discuss is that ROS are good at low and controlled levels; if an external insult disturbs the ROS homeostasis, they could be lethal for cells. That is what antimicrobial peptides do.

Here, *Mo*-CBP$_3$-PepII induced an uncontrolled accumulation of $\bullet O_2^-$ and H_2O_2 (Fig. 1). At higher levels, $\bullet O_2^-$ and H_2O_2 could cause severe damage to cells by interacting and degrading critical cellular components such as DNA, proteins, lipids, inducing membrane pore formation, apoptosis and death [16–20]. For example, higher levels of $\bullet O_2^-$ as demonstrated in Fig. 1, led to DNA oxidation mediated by iron [20]. High levels of $\bullet O_2^-$ increase free iron levels by releasing it from heme-oxidized proteins and enzyme clusters. The free iron interacts with DNA molecules oxidizing them and inducing fragmentation [20]. This result agrees with Aguiar et al. [10], that reported *Mo*-CBP$_3$-PepII induced DNA fragmentation in *C. neoformans* cells.

In the case of H_2O_2, higher levels of H_2O_2 drive the lipid peroxidation in the membrane and, thus, pore formation [18]. Recently, it was reported that two synthetic peptides, *Rc*Alb-PepII and PepGAT, lost the ability to induce pore formation in the *C. neoformans* membrane in the presence of an antioxidant agent where no H_2O_2 accumulation. This result suggests both peptides induce pore formation by ROS-dependent pathway [21]. Besides damaging the membrane, higher levels of H_2O_2 could also result in a higher level of oxidized protein and loss of activity. Proteomic analysis of

Klebsiella pneumoniae cells in the presence of a synthetic peptide *Mo*-CBP$_3$-PepI, which induced higher levels of H_2O_2, revealed an increase in the accumulation of proteins involved in the repair of oxidized proteins [22]. This data suggests that *K. pneumoniae* cells are trying to fix the damaged proteins by H_2O_2.

2.2. *Mo*-CBP$_3$-PepII affects the activity of redox system enzymes

Aguiar et al. [10] revealed *Mo*-CBP$_3$-PepII forms a 6-kDa pore in the membrane of *C. neoformans*. So, it was reasoned that *Mo*-CBP$_3$-pepII could move by this pore and interfere with the activity of some cytoplasmic enzymes involved in ROS metabolism, leading to ROS accumulation, as shown in Figure 1. As discussed above, ROS are essential to life but only if controlled to safer levels [12]. The safer levels of ROS were maintained by two mechanisms: enzymatic and non-enzymatic [23]. The enzymatic is mediated by scavenger enzymes that either convert highly unstable ROS molecules to more stable or completely oxidize them to H_2O and O_2 [23]. Here, the activity of three enzymes, SOD, CAT, and APX, was analyzed (Fig. 2).

The first enzyme analyzed was SOD because it is involved in the conversion of $\bullet O_2^-$ to H_2O_2 [24]. In control *C. neoformans* cells, the SOD activity was 5.67 AU mgP^{-1}. In contrast, no activity was detected in *Mo*-CBP$_3$-PepII-treated cells (Fig. 2A). In addition, two other enzymes were analyzed, CAT and APX, both involved in the conversion of H_2O_2 into H_2O in O_2 [25,26]. Regarding the CAT activity, control cells of *C. neoformans* presented an activity of 0.52 AU mgP^{-1} and *Mo*-CBP$_3$-PepII-treated cells showed a value of 0.121 AU mgP^{-1}. A reduction of 4.0-fold in CAT activity (Fig. 2B). The APX activity from *C. neoformans* cells was also affected by *Mo*-CBP$_3$-PepII (Fig. 3C). *Mo*-CBP$_3$-PepII (0.77 AU mgP^{-1}) induced a reduction of 4.5-fold in APX activity compared to control cells (3.40 AU mgP^{-1}) (Fig. 2C).

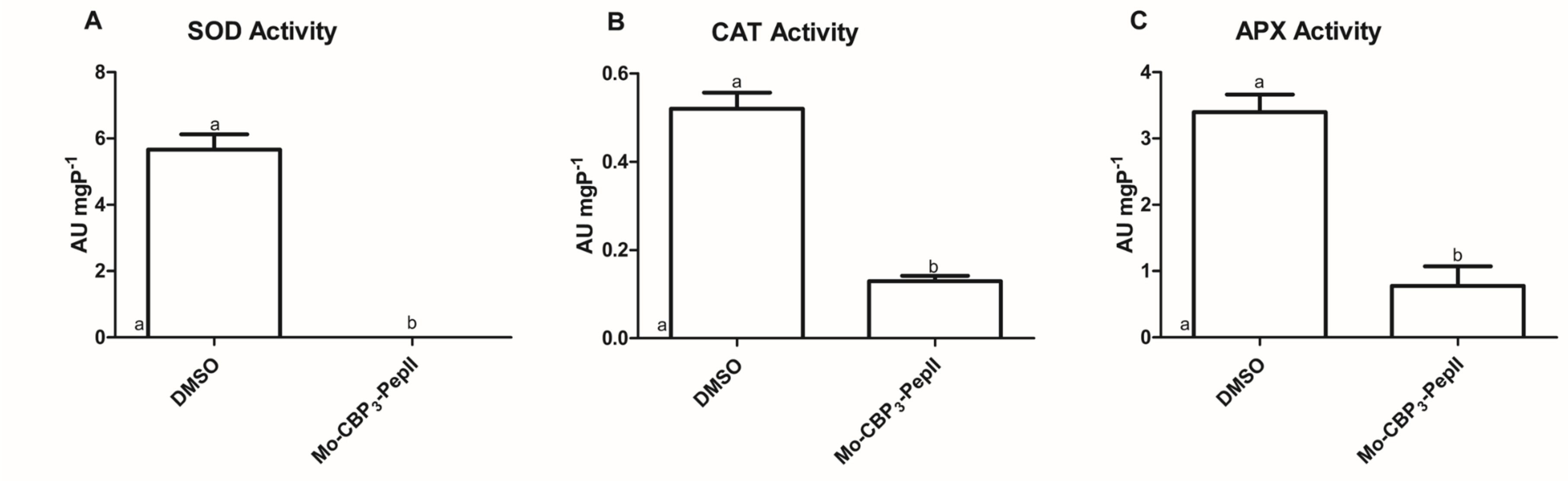

Figure 2. The activity of enzymes involved in ROS in *C. neoformans* cells after treatment with *Mo*-CBP$_3$-PepII. The activity of enzymes was tested in *C. neoformans* cells treated (*Mo*-CBP$_3$-PepII) and non-treated (DMSO) with the synthetic peptide. The different lowercase letters indicate statistical significance at $p > 0.05$.

As demonstrated in Fig. 2, *Mo*-CBP$_3$-PepII induced alteration in the activity of enzymes involved in the ROS scavenger process. By an unclear mechanism, *Mo*-CBP$_3$-PepII insults the balance of ROS in *C. neoformans* cells. First, the inhibition of SOD activity (Fig. 2A) agrees with the accumulation of $\bullet O_2^-$ (Fig. 1). Second, the reduction in the activity of CAT and APX let high the levels of H_2O_2 (Fig. 2B and C). The number of studies showing such alteration in redox enzymes is scarce. Two synthetic peptides, *Rc*Alb-PepII and *Rc*Alb-PepII, could also completely inhibit the SOD activity and reduce CAT and APX activities in *C. neoformans* cells, leading to ROS accumulation [21]. In another study, not with peptides but with an antifungal protein, *Mo*-CBP$_2$, purified from *Moringa oleifera* seeds, presented perturbation in the activity of those enzymes in *Candida albicans* [27].

This scenario strongly corroborates the previous results of *Mo*-CBP$_3$-PepII [10]. Recently, Aguiar et al. [10] *Mo*-CBP$_3$-PepII induced DNA fragmentation and apoptosis in *C. neoformans* cells. Altogether, previous results and those presented here showed a high accumulation of ROS in *C. neoformans* cells that could drive DNA fragmentation and apoptosis.

2.3. Ascorbic acid (AsA) affects the anticryptococcal potential of *Mo*-CBP$_3$-PepI

Figures 1 and 2 revealed *Mo*-CBP$_3$-PepII induced the overaccumulation of ROS by negatively modulating the activity of scavenger enzymes. These results correspond to previous damage caused by *Mo*-CBP$_3$-PepII in *C. neoformans* cells [10]. Based on that, one question emerged: is the activity of *Mo*-CBP$_3$-PepII ROS-dependent? To answer this question, *Mo*-CBP$_3$-PepII was assayed against *C. neoformans* in the presence of 10 mM of AsA. At the concentration of 25 µg mL^{-1}, *Mo*-CBP*3*-PepII reaches the MIC50 without

AsA (Fig. 3 – graphic). In the presence of 10 mM of AsA, the anticryptococcal activity of *Mo*-CBP$_3$-PepII dropped to 10%, a reduction of 40% in activity (Fig. 3 – graphic).

Aguiar et al. [10] reported that *Mo*-CBP$_3$-PepII could induce pore formation in membranes of *C. neoformans* cells, as revealed by the propidium iodide (PI) uptake assay. In the presence of AsA, fluorescence microscopy revealed no H_2O_2 accumulation and pore formation (Fig. 3), indicating that *Mo*-CBP$_3$-PepII lost the ability to induce pore formation. This result suggests the ability of *Mo*-CBP$_3$-PepII to induce pore formation is H_2O_2-dependent.

As happened to ROS, pore formation is also a common mechanism of action played by peptides because it could result from ROS accumulation and lipid peroxidation or the direct action of peptides in the membrane [18,28,29]. These data suggest the activity and mechanism of action of *Mo*-CBP3-PepII are dependent on ROS accumulation. This result is different from others presented by peptides RcAlb-PepIII and PepKAA [21], where the ability of pore formation is independent of ROS.

It seems that *Mo*-CBP$_3$-PepII first interacts with *C. neoformans* cells interfering with the ROS scavenger enzyme activity leading to the accumulation of ROS and, thus, several other damages to *C. neoformans,* driving them to death.

2.4. *Mo*-CBP$_3$-PepII interferes in the biosynthesis of ergosterol

Ergosterol is a fungal membrane component, and its primary function is acting as a stabilizer [30]. The biosynthesis of ergosterol occurs in the cytoplasm of the cell and is transported to the membrane [30]. Aguiar et al. [10] demonstrated that *Mo*-CBP$_3$-PepII was able to bind to ergosterol. Therefore, we experimented with evaluating the ability of *Mo*-CBP$_3$-PepII to inhibit the ergosterol synthesis (Fig. 4A). As expected, in control with DMSO-NaCl, there was no inhibition of ergosterol synthesis. The positive control for inhibition, itraconazole (ITR), was able to inhibit 47.65% of ergosterol biosynthesis (Fig. 4A). Meanwhile, *Mo*-CBP_3-PepII inhibited the ergosterol biosynthesis in 72% (Fig. 4A), a value 1.5 times higher than ITR.

By inhibiting the biosynthesis of ergosterol, *Mo*-CBP_3-PepII destabilizes the membrane facilitating the pore formation on the membrane leading to loss of cytoplasmic content and cell death. *Mo*-CBP_3-PepII targets ergosterol in two ways: interacting with it in the membrane [10] or inhibiting its synthesis in *C. neoformans* cells (Fig. 4A).

2.5 Energetic metabolism is affected in *C. neoformans* treated with *Mo*-CBP_3-PepII

Still looking for possible cytoplasmic targets of *Mo*-CBP_3-PepII, the lactate dehydrogenase (LDH) activity was assayed in *C. neoformans* cells after contact. The activity of LDH was wholly inhibited in cells treated with *Mo*-CBP_3-PepII (MIC_{50}) (Fig. 4B). As expected, control cells did not suffer any alteration in LDH activity (Fig. 4B).

LHD is an essential enzyme in carbohydrate metabolism because it is involved in the regeneration of NAD^+ from NADH produced in the glycolysis pathway. This reaction maintains a high ratio of NAD^+/NADH in the cytoplasm, favoring glycolysis [31]. By inhibiting the LDH activity, *Mo*-CBP_3-PepII interferes in the regeneration of NAD^+, which is essential for glycolysis still works. The inhibition of LDH can jeopardize all energetic metabolism in *C. neoformans* cells.

Another parameter of energetic metabolism evaluated was the decoupling of Cyt c from the mitochondrial membrane (Fig. 4C). In cells treated with *Mo*-CBP_3-PepII (MIC_{50}), there was a significant increase of 51% of Cyt *c* content in the cytoplasm. The positive control H_2O_2 promotes 100% of Cyt *c* release from mitochondrial to cytoplasm (Fig. 4C). DMSO did not promote any release of Cyt c. At that time, *Mo*-CBP_3-PepII is interfering with energy production in mitochondria. The release of Cyt c from the mitochondrial membrane impairs the complete function of the electron transport chain (ETC) in the mitochondrion leading to a depletion in ATP levels [32]. These analyses suggest *Mo*-CBP$_3$-PepII has targets within *C. neoformans* cells and might reach the cytoplasm and other organelles.

One fact is, *Mo*-CBP3-PepII affects the energy production of *C. neoformans* cells in both stages in the cytoplasm and mitochondria. Energy is critical for any organism to cope with stresses of any kind, for example, to produce defense proteins [33]. Here, we showed that *Mo*-CBP3-PepII imposes different types of stress on *C. neoformans* cells and shutting down the energy production mitigates the chances of *C. neoformans* fighting back.

The role in ETC is the canonical function of Cyt c. However, its role goes beyond that [32]. Cyt c is also crucial for the health of mitochondria. The decoupling of Cyt c from mitochondrial membranes signals mitochondrion misfunction and thus starts cell apoptosis [32]. Therefore, by inducing the release of o Cyt c from the mitochondrial membrane, *Mo*-CBP$_3$-PepII induces *C. neoformans* cells to enter apoptosis. Aguiar et al. [10] revealed that *Mo*-CBP$_3$-PepII induced apoptosis in *C. neoformans* cells corroborating the results reported here.

2.6 *Mo*-CBP$_3$-PepII promotes several changes in the cell structure of *C. neoformans*

Atomic force microscopy (AFM) analysis revealed the effects that *Mo*-CBP$_3$-PepII induces in the structure of *C. neoformans* cells. The control showed a cryptococcal cell in its morphology with no damage (Fig. 5A and B), healthy and continuous cytoplasmatic membrane, homogenous cytoplasm, and no damage to the capsule. By contrast, *C. neoformans* treated with *Mo*-CBP$_3$-PepII showed several damages in its structure, such as damage to the membrane, cell wall thickness, damage to fungal capsules, wrinkled cytoplasm, and roles across the whole cells (Fig. 5C and D – brown dots). Also, it is possible to see that *Mo*-CBP$_3$-PepII-treated cells have a diameter and height and hence higher volume than control cells indicating treated cells are bigger than control cells (Fig. 5 C and D). This result suggests that *Mo*-CBP$_3$-PepII induced pore formation in the *C. neoformans* membrane by changing its permeability. In that case, cells cannot control the osmotic potential. Additionally, 3D images (Fig. 5D) showed that *C. neoformans* cells treated with *Mo*-CBP$_3$-PepII are flattened, presenting structures like depression in the middle of the cell.

Recently, the morphology of *C. neoformans* treated with synthetic peptides was revealed by scanning electron microscopy [10]. In this study, authors revealed several damages to the cell structure; in some cases, those are similar to data presented in this study, but AFM analysis brought more details on the effect of *Mo*-CBP$_3$-PepII on *C. neoformans* cells. Similar AFM data on *C. neoformans* cells were reported by Ishida et al. [34] using silver nanoparticles. In the study, the authors reported that *C. neoformans* cells presented damage in the cell wall, cell capsule, and membrane.

2.7 Proteomic profile of *C. neoformans* treated with *Mo*-CBP$_3$-PepII

2.7.1 Overview

Proteomic analysis is an important technique to see the whole picture of a cell by evaluating the protein profile after treatment with peptides [35–39]. Proteomic analysis has already been employed to study the response of resistant pathogens such as *Clostridioides difficile* [37]. Regarding *C. neoformans*, proteomic analysis was employed to understand the changes in protein profile during the transition from planktonic to biofilm lifestyle [40]. As far as we know, no study has employed proteomics to analyze the *C. neoformans* response to antimicrobial peptides, reinforcing the pioneering of our work.

As shown above, *Mo*-CBP$_3$-PepII presented different mechanisms against *C. neoformans* cells. However, all of those are despite only the cell structure itself. After that, one new question arises: is *Mo*-CBP$_3$-PepII able to change the protein profile of *C. neoformans*? A proteomic analysis was performed to obtain the answer (Fig. 6, Table 1, and supplementary Tables 1 and 2).

Five hundred seventy-three proteins were identified (Fig. 6A, Table 1, and supplementary Tables 1 and 2). Of these, 265 were exclusively identified in control cells (Supplementary Table 1), 266 were exclusively detected in *Mo*-CBP$_3$-PepII-treated cells (Supplementary Table 2), and 42 were detected in both groups (Fig. 6A and Table 1).

The proteins identified in both groups were called overlapping proteins. For these proteins, fold-change was calculated based on the intensity of peptides for proteins in *Mo*-CBP$_3$-PepII-treated/control cells [41]. Proteins with a fold-change value ≥ 1.5 ($p < 0.05$, Tukey's test) [41] were called up-accumulated (increase in abundance). Proteins with a fold-change value of ≤ 0.5 ($p < 0.05$, Tukey's test) [41] were called down-accumulated (decrease in abundance). Proteins with a fold-change value ranging from 0.5 to 1.5 ($p < 0.05$, Tukey's test) were considered they did not change in abundance [41] (Table 1). Among the overlapping proteins, 10 were up-accumulated, and 05 were down-accumulated in *Mo*-CBP$_3$-PepII-treated cells compared to control cells (Fig. 6A and Table 1). Twenty-seven overlapping proteins did not change their accumulation in response to *Mo*-CBP$_3$-PepII treatment in *C. neoformans* cells (Fig. 6A and Table 1).

The overlapping proteins were classified based on gene ontology for molecular function and biological process (Fig. 6B and C). Regarding the molecular function, proteins were classified into 9 groups DNA and RNA Binding (14.28%), Hydrolase

(7.14%), Oxidoreductase (9.52%), Ligase (2.38%), Multifunctional enzyme (2.38%), Protein Binding (9.52%), Transport or Structural Activity (11.90%), Transferase (26.19%), and Unknown (16.66%) (Fig. 6B, Table 1).

The biological process also revealed 9 groups of proteins Amino acid metabolism (9.52%), Cell Function and Structure (21.42%), Energetic metabolism (9.52%), Lipid metabolism (4.76%), Nucleic acid metabolism (23.80%), Protein folding (9.52%), Regulation Factor or Signaling (4.76%), Transport (4.76%), and Unknown (11.90%) (Fig. 6C, Table 1).

2.7.2 DNA and RNA binding proteins

In this group, two isoforms, DNA topoisomerase I and DNA topoisomerase 2, were exclusively detected in the *C. neoformans* cells treated with *Mo*-CBP$_3$-PepII (Supplementary table 2). DNA topoisomerases are proteins that solve topological problems in DNA molecules, such as supercoiling and catenation [42,43]. Topoisomerases are a well-known target for antifungal drugs such as echinocandins [42]. Despite their function in regulating DNA torsion, topoisomerases are also involved in the repair of damaged DNA. The exclusive detection of two isoforms of topoisomerases in treated cells indicates *Mo*-CBP$_3$-PepII [44]. Additionally, Pommier et al. [44] reported topoisomerase I is induced during cellular stress to prevent DNA hence cell death mediated by apoptosis [44]. The increase of topoisomerase 1 suggests the *Mo*-CBP$_3$-PepII is inducing damage to DNA. It is trustworthy to notice that Aguiar et al. [10] revealed that *Mo*-CBP$_3$-PepII induced DNA fragmentation and apoptosis; maybe these processes are related to apoptosis in *C. neoformans* cells induced by *Mo*-CBP$_3$-PepII.

Another protein only identified in *Mo*-CBP3-PepII-treated *C. neoformans* cells was the Mitochondrial escape protein 2 (MET2) (Supplementary table 2). MET2 protein controls the escape of mitochondrial DNA during stress to prevent degradation [45,46]. Once mitochondria suffer any external insult that could lead to DNA damage, the MET2 proteins are involved in the protection, repair, or even DNA escape to prevent worse damage [45,46]. Here, the increase in the abundance of MET2 protein only in treated cells suggests that *Mo*-CBP$_3$-PepII attacks mitochondrial, which follows the results above-mentioned that *Mo*-CBP$_3$-PepII induces the decoupling of Cyt c from the mitochondrial membrane (Fig. 4C).

Yet, another protein that deserved attention, the clustered mitochondria protein (CMP), was only detected in the control cells and not in treated cells (Supplementary tables 1 and 2). The CMP in Fungi and many other eukaryotic organisms is essential for mitochondrial health and functioning [47–49]. The absence of CMP leads to misfunction of mitochondria interfering with the normal function of the cell. This result indicates that *Mo*-CBP$_3$-PepII caused several damages to the mitochondrion reflectin to the whole *C. neoformans* cell.

2.7.3 Ligase- and amino acid metabolism-related proteins

In the ligase group, one protein was found in both treated and non-treated *C. neoformans* cells, the carbamoyl-phosphate synthase (Table 1). The fold-change value, 0.07, indicates that carbamoyl-phosphate synthase (CPS) decreased in abundance after treatment with *Mo*-CBP$_3$-PepII (Table 1). The CPS protein is involved in the biosynthesis of arginine [50,51]. Arginine is an essential amino acid involved in protein synthesis and in many other physiological and biochemical processes [51]. Liu et al. [51] reported that a CPS-mutant of pathogenic fungi *Magnaporthe oryzae* cannot produce arginine and affect the pathogenicity and development processes. Here, reducing CPS protein in *C. neoformans* cells could lead to arginine depletion, affecting vital cellular processes and, ultimately, death. Another protein, the Arginine biosynthesis bifunctional protein, in

Preprints (www.preprints.org) | NOT PEER-REVIEWED | Posted: 20 January 2023 doi:10.20944/preprints202301.0373.v1

which two isoforms were exclusively from control cells, reinforces the hypothesis that *Mo*-CBP$_3$-PepII interferes in arginine biosynthesis in *C. neoformans* cells (Supplementary tables 1 and 2).

Proteomic analysis revealed many proteins involved in amino acid metabolism were only detected in control cells (supplementary table 1), such as Alanine-tRNA ligase, histidine biosynthesis trifunctional protein, C-1-tetrahydrofolate synthase, glycine dehydrogenase. After treatment with the peptide, the decrease in abundance in all those proteins indicates a shutdown in protein synthesis [52]. The inability of the cell to produce proteins after the treatment with a drug causes severe forms of stress and inhibits cells from responding to stresses leading to death [52]. An antifungal drug called sordarin inhibits protein synthesis in pathogenic yeasts [53]. However, many yeasts, including *C. neoformans,* are intrinsically resistant to sordarin, making this drug useless for treatment. Nowadays, there are no drugs available that affect the protein synthesis of Fungi, which makes more attractive the effect of *Mo*-CBP$_3$-PepII in inhibiting the protein synthesis of *C. neoformans*.

2.7.4 Oxidoreductase-related proteins

In this group, one protein, D-2-hydroxyglutarate-pyruvate transhydrogenase, presented a fold-change value indicating its up-accumulation of it after exposure of *C. neoformans* cells to *Mo*-CBP$_3$-PepII (Table 1). The D-2-hydroxyglutarate-pyruvate transhydrogenase is mainly involved in the metabolism of lactate and oxidation of NADH to produce NAD$^+$ in the absence of LDH activity [54,55]. In *Saccharomyces cerevisiae,* the D-2-hydroxyglutarate-pyruvate transhydrogenase, also known as minor D-LDH, catalyzes the conversion of D-2-hydroxyglutarate into α-ketoglutarate using FAD$^+$ as a cofactor, and pyruvate as the donor of electrons producing lactate. The α-ketoglutarate in the cytosol is rapidly converted into 2-hydroxyglutarate, which is degraded in the cytosol by D-2-hydroxyglutarate-pyruvate transhydrogenase consuming NADH restoring NAD^+ [54,55].

As shown before, the activity of LDH is inhibited in cells after treatment with *Mo*-CBP_3-PepII interfering in NAD^+ restoring and impairing the glycolysis to keep stand. The up-accumulation of D-2-hydroxyglutarate-pyruvate transhydrogenase suggests the *C. neoformans* cells are trying to find a way to continue with the glycolysis pathway by employing an alternative way to maintain acceptable levels of NAD^+ essential do glycolysis pathway.

2.7.5 Protein Binding-related proteins

By analyzing proteins in this group, an unexpected result was seen. Many proteins components of the 26S proteasome, such as 26S proteasome regulatory subunit RPN1, 26S proteasome regulatory subunit RPN5, U3 small nucleolar RNA-associated, ERAD-associated E3 ubiquitin-protein, Uba3-binding protein but2, Ubiquinone biosynthesis protein, were only detected in control cells being absent in treated cells (Supplementary tables 1 and 2). In eukaryotic cells, the proteasome is a multicomplex enzymatic system that plays a role in protein turnover and many other cell processes, such as development, growth, division, cell-cycle progression, and defense [56–58]. The misfunction of proteasome could trap cells in a cell-cycle arrest and, consequently, apoptosis [57].

Here, the proteomic analysis revealed many proteasome subunits present in control cells, which is essential to its function, disappeared after the treatment with *Mo*-CBP_3-PepII (Supplementary Table 2). This result suggests *that C. neoformans* do not have a functional proteasome and could start apoptosis. This idea agrees with the results of Aguiar et al. [10], where *Mo*-CBP_3-PepII induces apoptosis in *C. neoformans* cells.

Another protein unique from the control cell was ASI1 (Supplementary Table 1). The ASI1 is a nuclear inner membrane-attached protein involved in correctly maintaining

doi:10.20944/preprints202301.0373.v1

gene expression regulation [59–61]. The protein ASI1 is involved in the functional folding of a group of transcription factors known as Stp proteins. In the absence of ASI1, unprocessed forms of Stp proteins were produced, leading to cell failure in control gene expression, involved in ribosomal RNA (rRNA) production [61]. So, somehow *Mo*-CBP$_3$-PepII induces alteration in the expression of rRNA and consequently reduces ribosome in *C. neoformans* treated cells. This result agrees with the shutting down in protein synthesis discussed above.

2.7.6 Transferase-related proteins

Eleven proteins in this group presented overlapping in the treated and control cells (Table 1). Of these, 6 proteins were up-accumulated, and 5 did not change. First is the atypical kinase COQ8, with a fold-chance value of 1.81 (Table 1). The atypical kinase COQ8 is a mitochondrial protein involved in coenzyme Q (CoQ) biosynthesis [62,63]. CoQ is a molecule involved in at least two critical processes in eukaryotic cells: (1) acting as electron transport in ETC and (2) working as an antioxidant [62,63]. Here, we reasoned the increase in atypical kinase COQ8 to increase the CoQ levels is a response of *C. neoformans* cells to two stresses imposed by *Mo*-CBP$_3$-PepII. First, high production of CoQ could be involved in a repair process of ETC, which is affected by the decoupling of Cyt c from the mitochondrial membrane (Fig. 4C). As discussed above, the release of Cyt c from mitochondrial jeopardizes the ETC and depletes the ATP synthesis. Second, higher CoQ levels might be associated with its antioxidant activity as a defense against ROS overaccumulation induced by *Mo*-CBP$_3$-PepII (Fig. 1).

The threonylcarbamoyl-AMP synthase presented a fold-change of 8.81 (Table 1), one of the higher evaluated in *C. neoformans* cells treated with *Mo*-CBP$_3$-PepII. The threonylcarbamoyl-AMP synthase is an important enzyme involved in the production of threonylcarbamoyl-AMP, a central metabolite essential for biosynthesis L-threonine and a universal tRNA nucleoside N6-threonylcarbamoyl adenosine involved in the maturation of tRNA [64,65]. The increase of threonylcarbamoyl-AMP synthase might be an attempt of *C. neoformans* cells to overcome the reduction in protein synthesis, as suggested above.

The enzyme (2E.6E)-farnesyl diphosphate synthase (FPPS) presented a fold-change of 11.12 in treated cells compared to control cells (Table 1). The FPPS protein is a crucial enzyme involved in a central biochemical pathway for eukaryotic cells, the isoprenoid biosynthesis pathway [66–69]. The isoprenoid biosynthesis produces sesquiterpenes that supply the production of many essential metabolites such as ubiquinone, dolichols, and sterols; in our case, for fungi, the participation in sterols biosynthesis leads to ergosterol biosynthesis [66–69]. Here, it was reported that *Mo*-CBP$_3$-PepII inhibits 60% of the biosynthesis of ergosterol, which in turn compromises the health of cellular membranes [67–69]. Altogether, this high fold-change value of FPPS led us to hypothesize that *C. neoformans* is trying to compensate for the inhibition of ergosterol biosynthesis to alleviate the damage to the membrane keeping it healthy and functional.

Another protein that was up-accumulated in the treated cells compared to the control was the spindle assembly checkpoint kinase (SAC). The SAC is a signal protein that indicates the mistaken attachment of the mitotic spindle to the kinetochores of chromosomes [70–72]. The SAC protein is vital during the checkpoint in the cell cycle. SAC protein is essential to check the correct position of chromosomes during the transition of metaphase-to-anaphase. If something goes wrong in this process, SAC protein accumulates and negatively regulates the CDC20 inhibiting cell division to prevent duplicated chromosome separation. The cell cycle is stopped until chromosomes are correctly aligned to the spindle [70–72]. The higher accumulation of SAC proteins in *C. neoformans* cells treated with *Mo*-CBP$_3$-PepII indicates an inhibition of the cellular cycle, decreasing the rate of cell division and, thus, in the case of *C. neoformans*, infection and pathogenicity [70–72].

2.7.7 Transport or Structural Activity-related proteins

Most of the overlapping proteins in this group decrease in accumulation in treated/control cells (Table 1), including Low-affinity methionine permease. Methionine is an essential proteinogenic amino acid [73,74]. As an essential amino acid, cells cannot synthesize methionine and must obtain it from the environment. To do so, cells use transports attached to the membrane to collect amino acids [73,74]. The low-affinity methionine permease transporter is used by *C. neoformans* cells to collect methionine from the environment. The *Mo*-CBP$_3$-PepII-treated *C. neoformans* cells presented a decrease in abundance of this transporter, leading to a decrease of methionine concentration within the cell, interfering in protein synthesis [73,74].

Another transporter, histidine permease, also decreased in abundance in *C. neoformans* cells after exposure to *Mo*-CBP$_3$-PepII (Supplementary Table 1). As happens to methionine, histidine is a proteinogenic essential amino acid that has to be collected by cells from the environment [75–78]. However, otherwise, than methionine permease, histidine permease functions go beyond histidine transport. In Fungi, histidine permeases are essential to keep fungi safe, virulent, vigorous, and normal morphogenesis and development [77,78]. The absence of this protein in *C. neoformans* cells treated with *Mo*-CBP$_3$-PepII suggests that all processes developed by it are compromised, making it hard for the fungus to overcome stresses imposed by the peptide.

Another protein that decreased in abundance in *C. neoformans* cells exposure to *Mo*-CBP$_3$-PepII was the oligomycin resistance ATP-dependent permease YOR1 (Table 1). Oligomycin is a molecule produced by bacteria from the *Streptomyces* genus and is used as an antibiotic. Oligomycin binds to ATP synthase inhibiting ATP synthesis [79–81]. Over the years, pathogenic yeasts have developed resistance to oligomycin by producing oligomycin resistance ATP-dependent permease YOR1 [80]. Thus, the reduction in the abundance of oligomycin resistance ATP-dependent permease YOR1 suggests that *C. neoformans* cells became susceptible to oligomycin after treatment with *Mo*-CBP$_3$-PepII.

A similar result was recently published by Branco et al. [22], revealing that the treatment of *Klebsiella pneumoniae* cells with the *Mo*-CBP$_3$-PepI synthetic peptide also induces the reduction in three multidrug resistance proteins such as multidrug resistance protein MdtN, UPF0194 membrane protein YbhG, and multidrug resistance protein EmrK. This result suggests *Mo*-CBP$_3$-PepI increases the susceptibility of *K. pneumoniae* to drugs. The same result was found in *C. neoformans* after treatment with *Mo*-CBP$_3$-PepII.

The BNI4 protein with the highest fold-change of 66.18 shows its significant accumulation in *C. neoformans* cells after treatment with *Mo*-CBP$_3$-PepII (Table 1). The BNI4 protein is involved in the recruitment of chitin synthase to produce the chitin to be incorporated in the cell wall of the new buddy [82,83]. Yeasts divide by cytokinesis, a process where one cell divides itself in two [84]. During this process, the cell wall needs to be produced for two cells; for this process, chitin synthase has to be recruited by the BNI4 protein [82–84].

We have one hypothesis for this higher level of BNI4 protein. *Mo*-CB$_3$-PepII is a synthetic peptide designed from the sequence of a chitin-binding protein from *Moringa oleifera* seeds, Mo-CBP$_3$ [11]. Lima et al. [85] proved that *Mo*-CBP$_3$-PepII is a chitin-binding peptide and causes damage to the cell wall of *Candida albicans* by interacting with chitin. Scanning electron microscopy reported by Aguiar et al. [10] and AFM analysis done here (Fig. 5) strongly suggest that *Mo*-CBP$_3$-PepII also in *C. neoformans* cell wall. As such, we hypothesize that *Mo*-CBP$_3$-PepII might interact with chitin and thus interfere with producing cell walls for new buds. To cope with this insult, *C. neoformans* cells raised the levels of BNI4 as much as possible to recruit chitin synthase to produce cell wall for new buds.

In contrast to BNI4, coronin is the protein with the lowest fold-change value of 0.04 (Table 1) and thus decreases in abundance in *C. neoformans* cells treated with *Mo*-CBP$_3$-PepII. Coronin is a protein critical for cell structure because it interacts with actin filaments and microtubules, promoting cellular processes such as remodeling the cell cytoskeleton, cell motility, endocytosis, and phagocytosis [86–88]. In yeasts, Cai et al. [88] reported that coronin protects actin filaments from depolymerization keeping the cytoskeleton functional. In contrast, in coronin-mutant yeasts, the function of actin filaments and cytoskeleton are compromised [88]. Those coronin-mutant yeasts lost the ability to remodel the cytoskeleton as well as have other cytoskeleton-dependent functions compromised. Here, the dramatic reduction in the levels of coronin in peptide-treated *C. neoformans* cells suggests that *Mo*-CBP$_3$-PepII is affecting the well-function of the cytoskeleton and inhibiting critical processes to cell life.

2.7.8 Energetic metabolism-related proteins

The most exciting proteins were identified exclusively in *C. neoformans* cells treated com *Mo*-CBP$_3$-PepII (Supplementary Table 2). The first protein found was Cytochrome c mitochondrial import. The Cytochrome c mitochondrial import is a protein that imports the cytoplasmic cytochrome c to the mitochondrial membrane [89–92]. The exclusive identification of this protein in *C. neoformans* cells treated with *Mo*-CBP3-PepII is very exciting. As pointed out above, *Mo*-CBP$_3$-PepII induced the decoupling of

Cyt c from the mitochondrial membrane (Fig. 4C). Therefore, the exclusive identification of Cytochrome c mitochondrial import in *C. neoformans* treated cells indicates strongly suggests the cell is trying to respond to the stresses caused by peptide either by producing new Cyt c molecules or even recoupling the molecules released by the peptide.

Another protein exclusively identified in treated cells was alcohol dehydrogenase 4 (supplementary table 2). Alcohol dehydrogenase functions in the alcoholic fermentation of yeasts [93,94]. In alcohol fermentation, the pyruvate is produced in glycolysis. After glycolysis, pyruvate is driven to a two-reaction reaction, where it is converted into ethanol in a step catalyzed by alcohol dehydrogenase [93,94]. The point in the alcoholic formation is that, in the reduction of pyruvate to ethanol, the NADH cytosolic produced in the glycolysis is converted into $NAD^{+,}$ raising the ratio NAD^+/NADH and thus favoring the glycolysis [93,94].

The point is, in the *C. neoformans* treated cells, a reduction in the activity of LDH induced by *Mo*-CBP_3-PepII (Fig. 4A). LDH recovered the NAD^+ by lactic fermentation, keeping high the NAD^+/NADH ratio to favor glycolysis [31]. So, it is feasible to suggest that the high level of Alcohol dehydrogenase is an attempt of *C. neoformans* cells to compensate for the inhibition of LDH by *Mo*-CBP_3-PepII and stand high the NAD^+/NADH ratio to favor glycolysis.

2.7.9 Pathogenicity-related proteins

In this group, one protein exclusively detected in control cells and absent in the treated deserves attention, the Subtilisin-like protease 6 (Supplementary table 1 and table 2). The subtilisin-like proteases are enzymes in fungi autophagy and fungal virulence, enhancing invasion and colonization [95,96]. The absence of Subtilisin-like protease 6 after treatment with *Mo*-CBP_3-PepII (supplementary table 2) indicates the *C. neoformans* cells stay with a limited capacity to cause infection.

3. Conclusion

The results presented here showed that *Mo*-CBP$_3$-PepII displays its anticryptococcal activity by multiple mechanisms of action affecting several cellular processes essential for cell life, such as development, pathogenesis, cell division, and metabolism. Acting on cells in multiple ways, *Mo*-CBP$_3$-PepII difficult the development of resistance by *C. neoformans*. Additionally, our results suggest that *Mo*-CBP$_3$-PepII could act as an adjuvant for drugs that are becoming useless. Additionally, recent studies showed that *Mo*-CBP$_3$-PepII is a safe molecule presenting no toxicity to human erythrocytes, MRC-5, HaCAT, L292 human cell lines, and zebrafish embryos [11,97]. Therefore, it is feasible to suggest that *Mo*-CBP$_3$-PepII is a potential molecule to be employed alone or in combination with other drugs to develop new treatments against *C. neoformans*.

4. Materials and methods

4.1 Fungal strains, chemicals, and synthetic peptides

Cryptococcus neoformans (ATCC 32045) was obtained from the Department of Biochemistry and Molecular Biology at the Federal University of Ceará (UFC), Fortaleza, Brazil. All the chemicals used in the experiments were obtained from Sigma Aldrich (São Paulo, SP, Brazil). The *Mo*-CBP$_3$-PepII (NIQPPCRCC) synthetic peptide was chemically synthesized by the company ChemPeptide (Shanghai, China).

4.2 Antifungal assay

The antifungal assay was performed according to Aguiar et al. [10]. The cryptococcal cells were cultivated in yeast potato dextrose (YPD) agar for 10 days. Then cells were collected and transferred to a liquid YPD medium. The concentration of *Mo*-CBP$_3$-PepII was the MIC$_{50}$ (25 µg mL^{-1}) defined by Aguiar et al. [10]. This MIC$_{50}$ concentration was used in all experiments performed in this study. Therefore, 25 µL of *C. neoformans* cells (10^6 cells mL^{-1}) and 25 µL of *Mo*-CBP$_3$-PepII (25 µg mL^{-1}) were incubated for 24 h at 30 °C before each assay. DMSO-NaCl was the control used.

4.3 Detection of *Mo*-CBP$_3$-PepII-Induced Overproduction of ROS

Fluorescence microscopy assay was performed to evaluate the *Mo*-CBP$_3$-PepII-induced H2O2 overproduction, as described previously by Dias et al. [98]. After the antifungal assay (section 4.2), the samples were washed with 0.15 M NaCl and centrifugated (5000 × *g* 5 min at 4 °C) three times and then were incubated with 9 µL of 2′,7′ dichlorofluorescein diacetate (DCFH-DA, Sigma, St. Louis, MI, 364 USA) for 30 min in the dark at 22 ± 2 °C. Next, the samples were washed and centrifuged as mentioned, transferred to slides, and observed with a fluorescence microscope (Olympus System BX 41, Tokyo, Japan) with an excitation wavelength of 535 nm and 370 emission wavelength of 617 nm.

Additionally, the qualitative of anion superoxide was performed according to Choi et al. [99]. The antifungal assay was done as above. Then *C. neoformans* cells were washed, recovered in 0.15 M of NaCl, and incubated with 100 µM nitroblue tetrazolium chloride (NBT) (Sigma Aldrich, USA) for 2 hours at 22 ± 2 °C. Then, cells were washed to remove the excess NBT and visualized in a light microscope (Olympus System BX 41, Tokyo, Japan).

The experiments to evaluate the anticryptococcal activity in the presence of the antioxidant agent ascorbic were done following the methodology described by Neto et al. [27]. The experiments to perform the H_2O_2 overaccumulation and pore formation in ascorbic acid at 10 mM were performed as described by Aguiar et al. [21].

4.4 Protein Extraction from *C. neoformans* cells

The extraction of proteins from *C. neoformans* cells was done following Branco et al. [22]. After the antifungal assay, the samples were washed three times to remove the media with 50 mM Na^+-acetate pH 5.2 and centrifugated at 12,000 × *g* for 15 min at 4 °C. Then, samples were resuspended in 200 µL of extraction buffer and frozen at -20 °C for 24 h. After that, the samples were submitted to sonication for 30 min to break the cell wall and plasmatic membrane, centrifuged again, and the supernatant was collected. The Bradford assay [100] was performed to determine the protein concentration using bovine serum albumin (BSA). The extracted proteins were used for enzymatic assay and proteomic analysis.

4.5 Activity Redox system enzymes

4.5.1 *Ascorbate peroxidase (APX) activity*

To evaluate the APX activity, the methodology was performed according to Souza et al. [101]. In tubes, 100 µL of the treated or control samples were mixed with 800 µL of 50 mM K^+-phosphate buffer, pH 6.0, containing 0.5 mM of L-ascorbic acid and incubated at 30 °C for 10 minutes. Then, 100 µL of 2 mM H_2O_2 was added to start the reaction. The reaction was tracked every 10 seconds until 1 min in the spectrophotometer (Biochron, Libra 394 S12) at the wavelength 290 nm. APX activity unity (AU) was expressed as the reduction in the absorbance by 0.01 at 290 nm, indicating the use of ascorbate to remove H_2O_2 by milligram of the protein (UA mgP^{-1}).

4.5.2 *Catalase (CAT) activity*

Following Souza et al. [101], 200 µL of proteins extracted from *Mo*-CBP$_3$-PepII-treated and non-treated *C. neoformans* cells were incubated with 700 µL 50 mM K$^+$-phosphate buffer pH 7.0 at 30 °C for 10 min. Next, 100 µL of H_2O_2 was added to start the reaction. The reaction medium was transferred to a quartz cuvette (1 cm^{-1}), and the absorbance was measured in a spectrophotometer (Biochron, Libra 394 S12). The decrease in absorbance at 240 nm was observed at intervals of 10 seconds to 1 minute. CAT activity unity (AU) was expressed as the reduction in the absorbance by 0.01 at 240 nm, indicating the use of ascorbate to remove H_2O_2 by milligram of the protein (UA mgP^{-1}).

4.5.3 *Superoxide dismutase (SOD) activity*

SOD activity was performed following the methodology described by Souza et al. [101]. In a flat-bottom 96 well-plate was mixed 10 µL of 1 M K$^+$-phosphate buffer pH 7.8, 20 µL 1 mM 2,2',2'',2'''- ethylenediaminetetraacetic acid (EDTA), 10 µL of 0.25% Triton X-100, 20 µL of 130 mM L-Methionine, 100 µL of protein extract from *C. neoformans* cells in the presence and absence of *Mo*-CBP$_3$-PepII (MIC$_{50}$), 20 µL 100 mM of riboflavin, 20 µL of 700 µM of BNT. The mixture was homogenized and kept in the dark for 5 min. After that, the plate was exposed to a 32-W fluorescent light and the absorbances were measured in 1 min intervals up to 5 min at 630 nm in a microplate reader (Epoch, Biotek, Santa Clara, CA, USA). Blanks consisted of all reagents used without protein extracts, it was replaced with deionized water. The SOD was expressed in activity units per mg of protein (AU mgP^{-1}). One unit of SOD activity (1 AU) corresponded to the amount of the sample needed to inhibit the photoreduction of NBT by 50%.

4.6 Ergosterol inhibition synthesis

The inhibition of ergosterol biosynthesis was evaluated according to Neto et al. [27]. The *C. neoformans* cells were cultivated in the presence of *Mo*-CBP$_3$-PepII (MIC$_{50}$), 5% DMSO, and Itraconazole (ITR) (1000 μg mL^{-1}) for 24 h at 30 °C. Then, the cells were centrifugated at 3000 × *g* for 5 min. Subsequently, the pellet was dried and weighed. Two mL of 25% alcoholic sodium hydroxide solution (m/v) was added to each pellet and strongly vortexed for 1 min. To extract the sterol, 4 mL of sterile 75% n-hexane was added and vortexed for 3 min. Then, 400 µL of pure ethanol was added to 200 µL sterol extract. Next, the samples were transferred to a quartz cuvette (1 cm) and the absorbance was measured in a spectrophotometer (Biochron, Libra 394 S12) at 230 nm and 282 nm. Ergosterol content was calculated based on three equations:

Eq. 1: % ergosterol + 24(28) [DHE=(Abs282/290) x F] / pellet weight

Eq. 2: % 23(28) DHE =[(Abs230/518) x F] / pellet weight

Eq. 3: % ergosterol = % ergosterol + 24(28) DHE - % 24(28) DHE

24 (28) DHE refers to dehydroergosterol, where the absorbance is similar to ergosterol at 282 nm. F, in both equations, represents the factor of dilution of ethanol.

4.7 Lactate dehydrogenase (LDH) activity

The LDH Liquiform™ kit (Labtest Diagnóstica, BR) was measured according to the manufacturer's instructions.

4.8 Cytochrome c release

The assay was performed according to Neto et al. [27]. The cells were incubated with *Mo*-CBP$_3$-PepII (MIC$_{50}$), H_2O_2 (10 mM), and DMSO-NaCl for 24 h at 30 °C. Then, 100 µL of buffer 50 mM Tris-HCl pH 7.5 containing 2 mM EDTA, 1 mM phenylmethylsulphonyl fluoride, and 6% glucose were added to the cell suspension and homogenized. Subsequently, the samples were centrifuged at 2000 x g at 4 °C for 10 min and the supernatant was collected and added into microtubes. The pellet was washed with the buffer 50 mM Tris pH 7.5 containing 2 mM EDTA and centrifugated (6000 x g for 30 sec). The supernatant was discarded, and the mitochondria were suspended in 100 µL of the same buffer. Next, the cytosolic and mitochondrial suspensions were treated with 30 mM of ascorbic acid for 5 min at 30 °C. Then, the optical density of the obtained solution was measured using a microtiter plate reader (Epoch, Biotek, Santa Clara, CA, USA) at 550 nm.

4.9 Atomic Force Microscopy (AFM)

After the antifungal assay, the cells were prepared for AFM analysis following the methodology described by Souza et al. [102]. The samples were washed three times with sterile water and centrifugated at 5000 x g for 5 min at 4 °C. Then, 10 µL of the cells were transferred to a freshly washed glass surface previously treated with (v/v) poly-L-lysine and incubated at room temperature (22 ± 2°C) for 30 min. All samples were analyzed on Multimode 8 (Bruker, Santa Barbara, CA, USA). The probes used were SNL (Bruker) with 0.06 N/m nominal spring constant, a resonance frequency of 320 kHz, and a nominal tip radius of 8 nm.

4.10 Gel-Free Proteomic Analysis

For proteomic analysis, proteins were extracted as described in section 4.4. Subsequently, proteins from the control and treated cells were treated with 10 mM DTT and incubated for 1 h at 37 °C in the dark to reduce the proteins. Next, 15 mM iodoacetamide was added and incubated for 30 min in a dark room to alkylate the reduced proteins. Then, the proteins were digested using trypsin gold (Promega, Madison, WI, USA) to a final concentration of 1:20 (w/w) as described by manufacturers for 16 h at 37

°C. After that, the samples were dried in a speed vacuum (Eppendorf, Hamburg, Germany) for 3 h and analyzed by an ESI-QUAD-TOF mass spectrometer.

4.11 Protein identification

The protein identification was performed following Branco et al. [22]. Tandem mass spectra were exported as .pkl files and loaded in the MASCOT MS/MS ions search from MATRIX SCIENCE (https://www.matrixscience.com/cgi/search_form.pl?FORMVER=2&SEARCH=MIS, accessed on 10 November 2022) against UP2311_*S_cerevisiae* (protein database), UP219602_*F_oxysporum* (protein database), and SwissProt databases (protein database). The search was done by following parameters: fixed modifications to Carbamidomethyl (C), variable modifications to Oxidation (O); the peptide charge was set to 2+, 3+, and 4+; and the instrument was set to ESI-QUAD-TOF. The proteins identified were searched for in UNIPROT and separated into 3 sets: 1) unique from control for those only identified in control samples, 2) unique from the cells treated with *Mo*-CBP$_3$-PepII for those only identified in treated samples, and 3) *Mo*-CBP$_3$-PepII x control overlapping proteins.

The proteins with a fold-change value ≥ 1.5 ($p < 0.05$, Tukey's test) were up-accumulated (increased the abundance), and proteins with a fold-change value ≤ 0.5 ($p < 0.05$, Tukey's test) were down-accumulated (decreased the abundance) and considered for comparisons. Proteins with a fold-change value between 0.5 to 1.5 were considered that did not change. For each protein, its corresponding FASTA file was downloaded. The blast2go program (https://www.blast2go.com/, accessed on 25 November 2022) was used to categorize the proteins detected by Gene Ontology (GO) annotation according to Molecular function, Biological Activity, and subcellular location.

4.12 Statistical Analysis

All experiments were performed in triplicates. The statistical analyses were performed using GraphPad Prism (version 5.01) for Microsoft Windows. All data obtained in the assays were compared using the one-way analysis of variance (ANOVA), followed by the Tukey test ($p < 0.05$).

Author Contributions: All authors made substantial contributions. The conception and design of the study and acquisition of data, analysis, and interpretation were performed by T.K.B.A., N.A.S.N., F.I.R.G., C.D.T.F., F.P.M., R.F.C., C.S.N., L.M.R.A., R.S.-O., J.T.A.O., and P.F.N.S. Microscopic analyses were carried out by T.K.B.A., N.A.S.N., L.M.R.A., R.S.-O., and P.F.N.S. Writing and revision of the article were carried out by T.K.B.A. and P.F.N.S. Lastly, P.F.N.S. performed the final approval and submission. All authors have read and agreed to the published version of the manuscript.

Funding: Special thanks to CAPES for providing the postdoctoral grant to Pedro F. N. Souza (grant number 88887.318820/2019-00).

Institutional Review Board Statement: Not applicable.

Informed Consent Statement: Not applicable.

Data Availability Statement: The data supporting this study’s findings are available upon request from the corresponding author.

Acknowledgments: We are grateful to the staff of the central analytical facilities of UFC, Brazil.

Conflicts of Interest: The authors report no conflicts of interest.

References

1. Seiler, G.T.; Ostrosky-Zeichner, L. Investigational Agents for the Treatment of Resistant Yeasts and Molds. *Curr. Fungal Infect. Rep.* **2021**, *15*, 104–115, doi:10.1007/s12281-021-00419-5.
2. Stewart, A.G.; Paterson, D.L. How Urgent Is the Need for New Antifungals? *Expert Opin. Pharmacother.* **2021**, *22*, 1857–1870, doi:10.1080/14656566.2021.1935868.
3. Organization, W.H. WHO Fungal Priority Pathogens List to Guide Research, Development and Public Health Action 2022, 1–48.
4. Woo, Y.H.; Martinez, L.R. *Cryptococcus Neoformans* –Astrocyte Interactions: Effect on Fungal Blood Brain Barrier Disruption, Brain Invasion, and Meningitis Progression. *Crit. Rev. Microbiol.* **2021**, *47*, 206–223, doi:10.1080/1040841X.2020.1869178.
5. Coelho, C.; Casadevall, A. Cryptococcal Therapies and Drug Targets: The Old, the New and the Promising. *Cell. Microbiol.* **2016**, *18*, 792–799, doi:10.1111/cmi.12590.
6. Maligie, M.A.; Selitrennikoff, C.P. *Cryptococcus Neoformans* Resistance to Echinocandins: (1,3)β-Glucan Synthase Activity Is Sensitive to Echinocandins. *Antimicrob. Agents Chemother.* **2005**, *49*, 2851–2856, doi:10.1128/AAC.49.7.2851-2856.2005.
7. Souza, P.F.N.; Marques, L.S.M.; Oliveira, J.T.A.; Lima, P.G.; Dias, L.P.; Neto, N.A.S.; Lopes, F.E.S.; Sousa, J.S.; Silva, A.F.B.; Caneiro, R.F.; et al. Synthetic Antimicrobial Peptides: From Choice of the Best Sequences to Action Mechanisms. *Biochimie* **2020**, *175*, 132–145, doi:10.1016/j.biochi.2020.05.016.
8. Erak, M.; Bellmann-Sickert, K.; Els-Heindl, S.; Beck-Sickinger, A.G. Peptide Chemistry Toolbox – Transforming Natural Peptides into Peptide Therapeutics. *Bioorg. Med. Chem.* **2018**, *26*, 2759–2765, doi:10.1016/j.bmc.2018.01.012.
9. Kundu, R. Cationic Amphiphilic Peptides: Synthetic Antimicrobial Agents Inspired by Nature. *ChemMedChem* **2020**, *15*, 1887–1896, doi:10.1002/cmdc.202000301.
10. Aguiar, T.K.B.; Neto, N.A.S.; Freitas, C.D.T.; Silva, A.F.B.; Bezerra, L.P.; Malveira, E.A.; Branco, L.A.C.; Mesquita, F.P.; Goldman, G.H.; Alencar, L.M.R.; et al. Antifungal Potential of Synthetic Peptides against Cryptococcus Neoformans: Mechanism of Action Studies Reveal Synthetic Peptides Induce

Membrane–Pore Formation, DNA Degradation, and Apoptosis. *Pharmaceutics* **2022**, *14*, 1678, doi:10.3390/pharmaceutics14081678.

11. Oliveira, J.T.A.; Souza, P.F.N.; Vasconcelos, I.M.; Dias, L.P.; Martins, T.F.; Van Tilburg, M.F.; Guedes, M.I.F.; Sousa, D.O.B. Mo-CBP3-PepI, Mo-CBP3-PepII, and Mo-CBP3-PepIII Are Synthetic Antimicrobial Peptides Active against Human Pathogens by Stimulating ROS Generation and Increasing Plasma Membrane Permeability. *Biochimie* **2019**, *157*, 10–21, doi:10.1016/J.BIOCHI.2018.10.016.
12. Mittler, R. ROS Are Good. *Trends Plant Sci.* **2017**, *22*, 11–19, doi:10.1016/J.TPLANTS.2016.08.002.
13. Zhang, Z.; Chen, Y.; Li, B.; Chen, T.; Tian, S. Reactive Oxygen Species: A Generalist in Regulating Development and Pathogenicity of Phytopathogenic Fungi. *Comput. Struct. Biotechnol. J.* **2020**, *18,* 3344, doi:10.1016/J.CSBJ.2020.10.024.
14. Cho, J.; Hwang, I. sok; Choi, H.; Hwang, J.H.; Hwang, J.S.; Lee, D.G. The Novel Biological Action of Antimicrobial Peptides via Apoptosis Induction. *J. Microbiol. Biotechnol.* **2012**, *22*, 1457–1466, doi:10.4014/JMB.1205.05041.
15. do Nascimento Dias, J.; de Souza Silva, C.; de Araújo, A.R.; Souza, J.M.T.; de Holanda Veloso Júnior, P.H.; Cabral, W.F.; da Glória da Silva, M.; Eaton, P.; de Souza de Almeida Leite, J.R.; Nicola, A.M.; et al. Mechanisms of Action of Antimicrobial Peptides ToAP2 and NDBP-5.7 against Candida Albicans Planktonic and Biofilm Cells. *Sci. Rep.* **2020**, *10*, doi:10.1038/S41598-020-67041-2.
16. Cho, J.; Lee, D.G. Oxidative Stress by Antimicrobial Peptide Pleurocidin Triggers Apoptosis in Candida Albicans. *Biochimie* **2011**, *93*, 1873–1879, doi:10.1016/j.biochi.2011.07.011.
17. Maurya, I.K.; Pathak, S.; Sharma, M.; Sanwal, H.; Chaudhary, P.; Tupe, S.; Deshpande, M.; Chauhan, V.S.; Prasad, R. Antifungal Activity of Novel Synthetic Peptides by Accumulation of Reactive Oxygen Species (ROS) and Disruption of Cell Wall against Candida Albicans. *Peptides* **2011**, *32*, 1732–1740, doi:10.1016/J.PEPTIDES.2011.06.003.
18. Uhl, L.; Gerstel, A.; Chabalier, M.; Dukan, S. Hydrogen Peroxide Induced Cell Death: One or Two Modes of Action? *Heliyon* **2015**, *1*, doi:10.1016/J.HELIYON.2015.E00049.
19. Han, M.; Wang, R.; Ding, N.; Liu, X.; Zheng, N.; Fu, B.; Sun, L.; Gao, P. Reactive

Oxygen Species-Mediated Caspase-3 Pathway Involved in Cell Apoptosis of Karenia Mikimotoi Induced by Linoleic Acid. *Algal Res.* **2018**, *36*, 48–56, doi:10.1016/j.algal.2018.10.013.

20. Keyer, K.; Imlay, J.A. Superoxide Accelerates DNA Damage by Elevating Free-Iron Levels. *Proc. Natl. Acad. Sci. U. S. A.* **1996**, *93*, 13635, doi:10.1073/PNAS.93.24.13635.
21. Aguiar, T.K.B.; Neto, N.A.S.; Silva, R.R.S.; Freitas, C.D.T.; Mesquita, F.P.; Alencar, L.M.R.; Santos-oliveira, R.; Goldman, G.H.; Souza, P.F.N. Behind the Curtain : In Silico and In Vitro Experiments Brought to Light New Insights into the Anticryptococcal Action of Synthetic Peptides. **2023**, 1–18.
22. Branco, L.A.C.; Souza, P.F.N.; Neto, N.A.S.; Aguiar, T.K.B.; Silva, A.F.B.; Carneiro, R.F.; Nagano, C.S.; Mesquita, F.P.; Lima, L.B.; Freitas, C.D.T. New Insights into the Mechanism of Antibacterial Action of Synthetic Peptide Mo-CBP3-PepI against Klebsiella Pneumoniae. *Antibiotics* **2022**, *11*, 1753, doi:10.3390/antibiotics11121753.
23. Belozerskaya, T.A.; Gessler, N.N. Reactive Oxygen Species and the Strategy of Antioxidant Defense in Fungi: A Review. *Appl. Biochem. Microbiol.* **2007**, *43*, 506–515, doi:10.1134/S0003683807050031.
24. Asakura, H.; Kitahora, T. Antioxidants and Polyphenols in Inflammatory Bowel Disease: Ulcerative Colitis and Crohn Disease. *Polyphenols Prev. Treat. Hum. Dis.* **2018**, 279–292, doi:10.1016/B978-0-12-813008-7.00023-0.
25. Staerck, C.; Gastebois, A.; Vandeputte, P.; Calenda, A.; Larcher, G.; Gillmann, L.; Papon, N.; Bouchara, J.-P.; Fleury, M.J.J. Microbial Antioxidant Defense Enzymes. *Microb. Pathog.* **2017**, *110*, 56–65, doi:10.1016/j.micpath.2017.06.015.
26. Shigeoka, S.; Ishikawa, T.; Tamoi, M.; Miyagawa, Y.; Takeda, T.; Yabuta, Y.; Yoshimura, K. Regulation and Function of Ascorbate Peroxidase Isoenzymes. *J. Exp. Bot.* **2002**, *53*, 1305–1319, doi:10.1093/jexbot/53.372.1305.
27. da Silva Neto, J.X.; da Costa, H.P.S.; Vasconcelos, I.M.; Pereira, M.L.; Oliveira, J.T.A.; Lopes, T.D.P.; Dias, L.P.; Araújo, N.M.S.; Moura, L.F.W.G.; Van Tilburg, M.F.; et al. Role of Membrane Sterol and Redox System in the Anti-Candida Activity Reported for Mo-CBP2, a Protein from Moringa Oleifera Seeds. *Int. J. Biol. Macromol.* **2020**, *143*, 814–824, doi:10.1016/j.ijbiomac.2019.09.142.
28. Cirac, A.D.; Moiset, G.; Mika, J.T.; Koçer, A.; Salvador, P.; Poolman, B.; Marrink, S.J.; Sengupta, D. The Molecular Basis for Antimicrobial Activity of Pore-

Forming Cyclic Peptides. *Biophys. J.* **2011**, *100*, 2422, doi:10.1016/J.BPJ.2011.03.057.

29. Lipkin, R.; Lazaridis, T. Computational Studies of Peptide-Induced Membrane Pore Formation. *Philos. Trans. R. Soc. B Biol. Sci.* **2017**, *372*, doi:10.1098/RSTB.2016.0219.
30. Dupont, S.; Lemetais, G.; Ferreira, T.; Cayot, P.; Gervais, P.; Beney, L. Ergosterol Biosynthesis: A Fungal Pathway for Life on Land? *Evolution* **2012**, *66*, 2961–2968, doi:10.1111/J.1558-5646.2012.01667.X.
31. Farhana, A.; Lappin, S.L. Biochemistry, Lactate Dehydrogenase. *StatPearls* **2022**.
32. Ow, Y.L.P.; Green, D.R.; Hao, Z.; Mak, T.W. Cytochrome c: Functions beyond Respiration. *Nat. Rev. Mol. Cell Biol.* **2008**, *9*, 532–542, doi:10.1038/NRM2434.
33. Swan, C.L.; Sistonen, L. Cellular Stress Response Cross Talk Maintains Protein and Energy Homeostasis. *EMBO J.* **2015**, *34*, 267–269, doi:10.15252/EMBJ.201490757.
34. Ishida, K.; Cipriano, T.F.; Rocha, G.M.; Weissmüller, G.; Gomes, F.; Miranda, K.; Rozental, S. Silver Nanoparticle Production by the Fungus Fusarium Oxysporum: Nanoparticle Characterisation and Analysis of Antifungal Activity against Pathogenic Yeasts. *Mem. Inst. Oswaldo Cruz* **2014**, *109*, 220–228, doi:10.1590/0074-0276130269.
35. Wenzel, M.; Chiriac, A.I.; Otto, A.; Zweytick, D.; May, C.; Schumacher, C.; Gust, R.; Albada, H.B.; Penkova, M.; Krämer, U.; et al. Small Cationic Antimicrobial Peptides Delocalize Peripheral Membrane Proteins. *Proc. Natl. Acad. Sci. U. S. A.* **2014**, *111*, 1409–1418, doi:10.1073/pnas.1319900111.
36. Senges, C.H.R.; Stepanek, J.J.; Wenzel, M.; Raatschen, N.; Ay, Ü.; Märtens, Y.; Prochnow, P.; Hernández, M.V.; Yayci, A.; Schubert, B.; et al. Comparison of Proteomic Responses as Global Approach to Antibiotic Mechanism of Action Elucidation. *Antimicrob. Agents Chemother.* **2021**, *65*, doi:10.1128/AAC.01373-20.
37. Maaß, S.; Bartel, J.; Mücke, P.A.; Schlüter, R.; Sura, T.; Zaschke-Kriesche, J.; Smits, S.H.J.; Becher, D. Proteomic Adaptation of Clostridioides Difficile to Treatment with the Antimicrobial Peptide Nisin. *Cells* **2021**, *10*, 1–21, doi:10.3390/cells10020372.
38. Tsakou, F.; Jersie-Christensen, R.; Jenssen, H.; Mojsoska, B. The Role of Proteomics in Bacterial Response to Antibiotics. *Pharmaceuticals* **2020**, *13*, 1–27,

doi:10.3390/ph13090214.

39. Moyer, T.B.; Purvis, A.L.; Wommack, A.J.; Hicks, L.M. Proteomic Response of Escherichia Coli to a Membrane Lytic and Iron Chelating Truncated Amaranthus Tricolor Defensin. *BMC Microbiol.* **2021**, *21*, 1–12, doi:10.1186/s12866-021-02176-4.
40. Santi, L.; Beys-Da-Silva, W.O.; Berger, M.; Calzolari, D.; Guimarães, J.A.; Moresco, J.J.; Yates, J.R. Proteomic Profile of Cryptococcus Neoformans Biofilm Reveals Changes in Metabolic Processes. *J. Proteome Res.* **2014**, *13*, 1545–1559, doi:10.1021/PR401075F.
41. Noronha Souza, P.F.; Abreu Oliveira, J.T.; Vasconcelos, I.M.; Magalhães, V.G.; Albuquerque Silva, F.D.; Guedes Silva, R.G.; Oliveira, K.S.; Franco, O.L.; Gomes Silveira, J.A.; Leite Carvalho, F.E. H2O2Accumulation, Host Cell Death and Differential Levels of Proteins Related to Photosynthesis, Redox Homeostasis, and Required for Viral Replication Explain the Resistance of EMS-Mutagenized Cowpea to Cowpea Severe Mosaic Virus. *J. Plant Physiol.* **2020**, *245*, 153110, doi:10.1016/j.jplph.2019.153110.
42. Shen, L.L.; Baranowski, J.; Fostel, J.; Montgomery, D.A.; Lartey, P.A. DNA Topoisomerases from Pathogenic Fungi: Targets for the Discovery of Antifungal Drugs. *Antimicrob. Agents Chemother.* **1992**, *36*, 2778–2784, doi:10.1128/AAC.36.12.2778.
43. Costa-Silva, H.M.; Resende, B.C.; Umaki, A.C.S.; Prado, W.; da Silva, M.S.; Virgílio, S.; Macedo, A.M.; Pena, S.D.J.; Tahara, E.B.; Tosi, L.R.O.; et al. DNA Topoisomerase 3α Is Involved in Homologous Recombination Repair and Replication Stress Response in Trypanosoma Cruzi. *Front. cell Dev. Biol.* **2021**, *9*, doi:10.3389/FCELL.2021.633195.
44. Pommier, Y.; Redon, C.; Rao, V.A.; Seiler, J.A.; Sordet, O.; Takemura, H.; Antony, S.; Meng, L.H.; Liao, Z.Y.; Kohlhagen, G.; et al. Repair of and Checkpoint Response to Topoisomerase I-Mediated DNA Damage. *Mutat. Res. - Fundam. Mol. Mech. Mutagen.* **2003**, *532*, 173–203, doi:10.1016/j.mrfmmm.2003.08.016.
45. Saita, S.; Shirane, M.; Nakayama, K.I. Selective Escape of Proteins from the Mitochondria during Mitophagy. *Nat. Commun. 2013 41* **2013**, *4*, 1–14, doi:10.1038/ncomms2400.
46. Pérez-Treviño, P.; Velásquez, M.; García, N. Mechanisms of Mitochondrial DNA

Escape and Its Relationship with Different Metabolic Diseases. *Biochim. Biophys. Acta - Mol. Basis Dis.* **2020**, *1866*, 165761, doi:10.1016/J.BBADIS.2020.165761.

47. Huang, P.; Yu, T.; Yoon, Y. Mitochondrial Clustering Induced by Overexpression of the Mitochondrial Fusion Protein Mfn2 Causes Mitochondrial Dysfunction and Cell Death. *Eur. J. Cell Biol.* **2007**, *86*, 289–302, doi:10.1016/J.EJCB.2007.04.002.
48. Fields, S.D.; Arana, Q.; Heuser, J.; Clarke, M. Mitochondrial Membrane Dynamics Are Altered in CluA- Mutants of Dictyostelium. *J. Muscle Res. Cell Motil.* **2002**, *23*, 829–838, doi:10.1023/A:1024492031696.
49. Zhu, Q.; Hulen, D.; Liu, T.; Clarke, M. The CluA- Mutant of Dictyostelium Identifies a Novel Class of Proteins Required for Dispersion of Mitochondria. *Proc. Natl. Acad. Sci. U. S. A.* **1997**, *94*, 7308–7313, doi:10.1073/PNAS.94.14.7308.
50. Nicoloff, H.; Hubert, J.C.; Bringel, F. In Lactobacillus Plantarum, Carbamoyl Phosphate Is Synthesized by Two Carbamoyl-Phosphate Synthetases (CPS): Carbon Dioxide Differentiates the Arginine-Repressed from the Pyrimidine-Regulated CPS. *J. Bacteriol.* **2000**, *182*, 3416–3422, doi:10.1128/JB.182.12.3416-3422.2000.
51. Liu, X.; Cai, Y.; Zhang, X.; Zhang, H.; Zheng, X.; Zhang, Z. Carbamoyl Phosphate Synthetase Subunit MoCpa2 Affects Development and Pathogenicity by Modulating Arginine Biosynthesis in Magnaporthe Oryzae. *Front. Microbiol.* **2016**, *7*, doi:10.3389/FMICB.2016.02023.
52. W, P.; CG, P.; G, M. Shut-down of Translation, a Global Neuronal Stress Response: Mechanisms and Pathological Relevance. *Curr. Pharm. Des.* **2007**, *13*, 1887–1902, doi:10.2174/138161207780858401.
53. Domínguez, J.M.; Kelly, V.A.; Kinsman, O.S.; Marriott, M.S.; Gómez De Las Heras, F.; Martín, J.J. Sordarins: A New Class of Antifungals with Selective Inhibition of the Protein Synthesis Elongation Cycle in Yeasts. *Antimicrob. Agents Chemother.* **1998**, *42*, 2274–2278, doi:10.1128/AAC.42.9.2274.
54. Signalling between Mitochondria and the Nucleus Regulates the Expression of a New D-lactate Dehydrogenase Activity in Yeast - Chelstowska - 1999 - Yeast - Wiley Online Library Available online: https://onlinelibrary.wiley.com/doi/pdf/10.1002/%28SICI%291097-0061%2819990930%2915%3A13%3C1377%3A%3AAID-

YEA473%3E3.0.CO%3B2-0 (accessed on 17 January 2023).

55. Becker-Kettern, J.; Paczia, N.; Conrotte, J.F.; Kay, D.P.; Guignard, C.; Jung, P.P.; Linster, C.L. Saccharomyces Cerevisiae Forms D-2-Hydroxyglutarate and Couples Its Degradation to d-Lactate Formation via a Cytosolic Transhydrogenase. *J. Biol. Chem.* **2016**, *291*, 6036–6058, doi:10.1074/JBC.M115.704494.
56. DH, L.; AL, G. Proteasome Inhibitors: Valuable New Tools for Cell Biologists. *Trends Cell Biol.* **1998**, *8*, 397–403, doi:10.1016/S0962-8924(98)01346-4.
57. Adams, J. The Proteasome: Structure, Function, and Role in the Cell. *Cancer Treat. Rev.* **2003**, *29*, 3–9, doi:10.1016/S0305-7372(03)00081-1.
58. Tanaka, K. The Proteasome: Overview of Structure and Functions. *Proc. Jpn. Acad. Ser. B. Phys. Biol. Sci.* **2009**, *85*, 12, doi:10.2183/PJAB.85.12.
59. Duan, C.G.; Wang, X.; Zhang, L.; Xiong, X.; Zhang, Z.; Tang, K.; Pan, L.; Hsu, C.C.; Xu, H.; Tao, W.A.; et al. A Protein Complex Regulates RNA Processing of Intronic Heterochromatin-Containing Genes in Arabidopsis. *Proc. Natl. Acad. Sci. U. S. A.* **2017**, *114*, E7377–E7384, doi:10.1073/PNAS.1710683114/SUPPL_FILE/PNAS.1710683114.SD01.XLSX.
60. Calvanese, E.; Gu, Y. Towards Understanding Inner Nuclear Membrane Protein Degradation in Plants. *J. Exp. Bot.* **2022**, *73*, 2266–2274, doi:10.1093/JXB/ERAC037.
61. Zargari, A.; Boban, M.; Heessen, S.; Andréasson, C.; Thyberg, J.; Ljungdahl, P.O. Inner Nuclear Membrane Proteins Asi1, Asi2, and Asi3 Function in Concert to Maintain the Latent Properties of Transcription Factors Stp1 and Stp2. *J. Biol. Chem.* **2007**, *282*, 594–605, doi:10.1074/JBC.M609201200.
62. Awad, A.M.; Nag, A.; Pham, N.V.B.; Bradley, M.C.; Jabassini, N.; Nathaniel, J.; Clarke, C.F. Intragenic Suppressor Mutations of the COQ8 Protein Kinase Homolog Restore Coenzyme Q Biosynthesis and Function in Saccharomyces Cerevisiae. *PLoS One* **2020**, *15*, doi:10.1371/JOURNAL.PONE.0234192.
63. Clarke, C.F. Insights into an Ancient Atypical Kinase Essential for Biosynthesis of Coenzyme Q. *Cell Chem. Biol.* **2018**, *25*, 123–125, doi:10.1016/J.CHEMBIOL.2018.02.001.
64. Harris, K.A.; Bobay, B.G.; Sarachan, K.L.; Sims, A.F.; Bilbille, Y.; Deutsch, C.; Iwata-Reuyl, D.; Agris, P.F. NMR-Based Structural Analysis of Threonylcarbamoyl-AMP Synthase and Its Substrate Interactions. *J. Biol. Chem.* **2015**, *290*, 20032–20043, doi:10.1074/JBC.M114.631242.

65. Swinehart, W.; Deutsch, C.; Sarachan, K.L.; Luthra, A.; Bacusmo, J.M.; de Crécy-Lagard, V.; Swairjo, M.A.; Agris, P.F.; Iwata-Reuyl, D. Specificity in the Biosynthesis of the Universal TRNA Nucleoside N6-Threonylcarbamoyl Adenosine (T6A)—TsaD Is the Gatekeeper. *RNA* **2020**, *26*, 1094–1103, doi:10.1261/RNA.075747.120.
66. Kim, H.Y.; Kim, D.K.; Bae, S.H.; Gwak, H.R.; Jeon, J.H.; Kim, J.K.; Lee, B. Il; You, H.J.; Shin, D.H.; Kim, Y.H.; et al. Farnesyl Diphosphate Synthase Is Important for the Maintenance of Glioblastoma Stemness. *Exp. Mol. Med.* **2018**, *50*, doi:10.1038/S12276-018-0166-2.
67. Fernandez, S.M.S.; Kellogg, B.A.; Poulter, C.D. Farnesyl Diphosphate Synthase. Altering the Catalytic Site to Select for Geranyl Diphosphate Activity. *Biochemistry* **2000**, *39*, 15316–15321, doi:10.1021/BI0014305.
68. Thulasiram, H. V.; Poulter, C.D. Farnesyl Diphosphate Synthase: The Art of Compromise between Substrate Selectivity and Stereoselectivity. *J. Am. Chem. Soc.* **2006**, *128*, 15819–15823, doi:10.1021/JA065573B.
69. Dhar, M.K.; Koul, A.; Kaul, S. Farnesyl Pyrophosphate Synthase: A Key Enzyme in Isoprenoid Biosynthetic Pathway and Potential Molecular Target for Drug Development. *N. Biotechnol.* **2013**, *30*, 114–123, doi:10.1016/j.nbt.2012.07.001.
70. Szymiczek, A.; Carbone, M.; Pastorino, S.; Napolitano, A.; Tanji, M.; Minaai, M.; Pagano, I.; Mason, J.M.; Pass, H.I.; Bray, M.R.; et al. Inhibition of the Spindle Assembly Checkpoint Kinase Mps-1 as a Novel Therapeutic Strategy in Malignant Mesothelioma. *Oncogene* **2017**, *36*, 6501–6507, doi:10.1038/ONC.2017.266.
71. Maia, A.R.R.; De Man, J.; Boon, U.; Janssen, A.; Song, J.Y.; Omerzu, M.; Sterrenburg, J.G.; Prinsen, M.B.W.; Willemsen-Seegers, N.; De Roos, J.A.D.M.; et al. Inhibition of the Spindle Assembly Checkpoint Kinase TTK Enhances the Efficacy of Docetaxel in a Triple-Negative Breast Cancer Model. *Ann. Oncol. Off. J. Eur. Soc. Med. Oncol.* **2015**, *26*, 2180–2192, doi:10.1093/ANNONC/MDV293.
72. Marston, A.L.; Wassmann, K. Multiple Duties for Spindle Assembly Checkpoint Kinases in Meiosis. *Front. Cell Dev. Biol.* **2017**, *5*, 109, doi:10.3389/FCELL.2017.00109/BIBTEX.
73. Kitajima, K.T.; Chiba, Y.; Jigami, Y. Mutation of High-Affinity Methionine Permease Contributes to Selenomethionyl Protein Production in Saccharomyces Cerevisiae. *Appl. Environ. Microbiol.* **2010**, *76*, 6351–6359, doi:10.1128/AEM.01026-10.

74. Chaumontet, C.; Azzout-Marniche, D.; Blais, A.; Piedcoq, J.; Tomé, D.; Gaudichon, C.; Even, P.C. Low-Protein and Methionine, High-Starch Diets Increase Energy Intake and Expenditure, Increase FGF21, Decrease IGF-1, and Have Little Effect on Adiposity in Mice. *Am. J. Physiol. Regul. Integr. Comp. Physiol.* **2019**, *316*, R486–R501, doi:10.1152/AJPREGU.00316.2018.

75. Li, D.; Agrellos, O.A.; Calderone, R. Histidine Kinases Keep Fungi Safe and Vigorous. *Curr. Opin. Microbiol.* **2010**, *13*, 424–430, doi:10.1016/J.MIB.2010.04.007.

76. Defosse, T.A.; Sharma, A.; Mondal, A.K.; de Bernonville, T.D.; Latgé, J.P.; Calderone, R.; Giglioli-Guivarc’h, N.; Courdavault, V.; Clastre, M.; Papon, N. Hybrid Histidine Kinases in Pathogenic Fungi. *Mol. Microbiol.* **2015**, *95*, 914–924, doi:10.1111/MMI.12911.

77. Nostadt, R.; Hilbert, M.; Nizam, S.; Rovenich, H.; Wawra, S.; Martin, J.; Küpper, H.; Mijovilovich, A.; Ursinus, A.; Langen, G.; et al. A Secreted Fungal Histidine- and Alanine-Rich Protein Regulates Metal Ion Homeostasis and Oxidative Stress. *New Phytol.* **2020**, *227*, 1174–1188, doi:10.1111/NPH.16606.

78. Doige, C.A.; Ames, G.F.L. ATP-Dependent Transport Systems in Bacteria and Humans: Relevance to Cystic Fibrosis and Multidrug Resistance. *Annu. Rev. Microbiol.* **1993**, *47*, 291–319, doi:10.1146/annurev.mi.47.100193.001451.

79. Hundal, T.; Norling, B.; Ernster, L. The Oligomycin Sensitivity Conferring Protein (OSCP) of Beef Heart Mitochondria: Studies of Its Binding to F1 and Its Function. *J. Bioenerg. Biomembr.* **1984**, *16*, 535–550, doi:10.1007/BF00743244.

80. Parker, J.H.; Trimble, I.R.; Mattoon, J.R. Oligomycin Resistance in Normal and Mutant Yeast. *Biochem. Biophys. Res. Commun.* **1968**, *33*, 590–595, doi:10.1016/0006-291X(68)90336-7.

81. Devenish, R.J.; Prescott, M.; Boyle, G.M.; Nagley, P. The Oligomycin Axis of Mitochondrial ATP Synthase: OSCP and the Proton Channel. *J. Bioenerg. Biomembr.* **2000**, *32*, 507–515, doi:10.1023/A:1005621125812.

82. Kozubowski, L.; Panek, H.; Rosenthal, A.; Bloecher, A.; DeMarini, D.J.; Tatchell, K. A Bni4-Glc7 Phosphatase Complex That Recruits Chitin Synthase to the Site of Bud Emergence. *Mol. Biol. Cell* **2003**, *14*, 26–39, doi:10.1091/MBC.E02-06-0373.

83. Larson, J.R.; Kozubowski, L.; Tatchell, K. Changes in Bni4 Localization Induced by Cell Stress in Saccharomyces Cerevisiae. *J. Cell Sci.* **2010**, *123*, 1050–1059,

doi:10.1242/JCS.066258.

84. Marchant, R.; Smith, D.G. Bud Formation in Saccharomyces Cerevisiae and a Comparison with the Mechanism of Cell Division in Other Yeasts. *J. Gen. Microbiol.* **1968**, *53*, 163–169, doi:10.1099/00221287-53-2-163/CITE/REFWORKS.
85. Lima, P.G.; Souza, P.F.N.; Freitas, C.D.T.; Oliveira, J.T.A.; Dias, L.P.; Neto, J.X.S.; Vasconcelos, I.M.; Lopes, J.L.S.; Sousa, D.O.B. Anticandidal Activity of Synthetic Peptides: Mechanism of Action Revealed by Scanning Electron and Fluorescence Microscopies and Synergism Effect with Nystatin. *J. Pept. Sci.* **2020**, 1–13, doi:10.1002/psc.3249.
86. Gandhi, M.; Goode, B.L. Coronin: The Double-Edged Sword of Actin Dynamics. *Subcell. Biochem.* **2008**, *48*, 72–87, doi:10.1007/978-0-387-09595-0_7.
87. Cai, L.; Makhov, A.M.; Bear, J.E. F-Actin Binding Is Essential for Coronin 1B Function in Vivo. *J. Cell Sci.* **2007**, *120*, 1779–1790, doi:10.1242/JCS.007641.
88. Cai, L.; Marshall, T.W.; Uetrecht, A.C.; Schafer, D.A.; Bear, J.E. Coronin 1B Coordinates Arp2/3 Complex and Cofilin Activities at the Leading Edge. *Cell* **2007**, *128*, 915–929, doi:10.1016/J.CELL.2007.01.031.
89. Nicholson, D.W.; Neupert, W. Import of Cytochrome c into Mitochondria: Reduction of Heme, Mediated by NADH and Flavin Nucleotides, Is Obligatory for Its Covalent Linkage to Apocytochrome C. *Proc. Natl. Acad. Sci. U. S. A.* **1989**, *86*, 4340–4344, doi:10.1073/PNAS.86.12.4340.
90. Dumont, M.E.; Cardillo, T.S.; Hayes, M.K.; Sherman, F. Role of Cytochrome c Heme Lyase in Mitochondrial Import and Accumulation of Cytochrome c in Saccharomyces Cerevisiae. *Mol. Cell. Biol.* **1991**, *11*, 5487–5496, doi:10.1128/MCB.11.11.5487-5496.1991.
91. Dumont, M.E. Mitochondrial Import of Cytochrome C. *Adv. Mol. Cell Biol.* **1996**, *17*, 103–126, doi:10.1016/S1569-2558(09)60011-4.
92. NICHOLSON, D.W.; KÖHLER, H.; NEUPERT, W. Import of Cytochrome c into Mitochondria. Cytochrome c Heme Lyase. *Eur. J. Biochem.* **1987**, *164*, 147–157, doi:10.1111/J.1432-1033.1987.TB11006.X.
93. Plapp, B. V.; Green, D.W.; Sun, H.W.; Park, D.H.; Kim, K. Substrate Specificity of Alcohol Dehydrogenases. *Adv. Exp. Med. Biol.* **1993**, *328*, 391–400, doi:10.1007/978-1-4615-2904-0_41/COVER.
94. Reid, M.F.; Fewson, C.A. Molecular Characterization of Microbial Alcohol

Dehydrogenases. *Crit. Rev. Microbiol.* **1994**, *20*, 13–56, doi:10.3109/10408419409113545.

95. Fu, H.; Chung, K.R.; Liu, X.; Li, H. Aaprb1, a Subtilsin-like Protease, Required for Autophagy and Virulence of the Tangerine Pathotype of Alternaria Alternata. *Microbiol. Res.* **2020**, *240*, 126537, doi:10.1016/J.MICRES.2020.126537.
96. Bryant, M.K.; Schardl, C.L.; Hesse, U.; Scott, B. Evolution of a Subtilisin-like Protease Gene Family in the Grass Endophytic Fungus Epichlo Festucae. *BMC Evol. Biol.* **2009**, *9*, 1–13, doi:10.1186/1471-2148-9-168/FIGURES/5.
97. Souza, P.F.N.; vanTilburg, M.F.; Mesquita, F.P.; Amaral, J.L.; Lima, L.B.; Montenegro, R.C.; Lopes, F.E.S.; Martins, R.X.; Vieira, L.; Farias, D.F.; et al. Neutralizing Effect of Synthetic Peptides toward SARS-CoV-2. *ACS Omega* **2022**, *7*, 16222–16234, doi:10.1021/acsomega.2c02203.
98. Dias, L.P.; Souza, P.F.N.; Oliveira, J.T.A.; Vasconcelos, I.M.; Araújo, N.M.S.; Tilburg, M.F. V; Guedes, M.I.F.; Carneiro, R.F.; Lopes, J.L.S.; Sousa, D.O.B. RcAlb-PepII, a Synthetic Small Peptide Bioinspired in the 2S Albumin from the Seed Cake of Ricinus Communis, Is a Potent Antimicrobial Agent against Klebsiella Pneumoniae and Candida Parapsilosis. *Biochim. Biophys. Acta - Biomembr.* **2020**, *1862*, 183092, doi:10.1016/j.bbamem.2019.183092.
99. Choi, H.S.; Kim, J.W.; Cha, Y.; Kim, C. A Quantitative Nitroblue Tetrazolium Assay for Determining Intracellular Superoxide Anion Production in Phagocytic Cells. *J. Immunoass. Immunochem.* **2006**, *27*, 31–44, doi:10.1080/15321810500403722.
100. MM, B. A Rapid and Sensitive Method for the Quantitation of Microgram Quantities of Protein Utilizing the Principle of Protein-Dye Binding. *Anal. Biochem.* **1976**, *72*, 248–254, doi:10.1006/ABIO.1976.9999.
101. Souza, P.F.N.; Silva, F.D.A.; Carvalho, F.E.L.; Silveira, J.A.G.; Vasconcelos, I.M.; Oliveira, J.T.A. Photosynthetic and Biochemical Mechanisms of an EMS-Mutagenized Cowpea Associated with Its Resistance to Cowpea Severe Mosaic Virus. *Plant Cell Rep.* **2017**, *36*, 219–234, doi:10.1007/s00299-016-2074-z.
102. Souza, P.F.N.; Vasconcelos, I.M.; Silva, F.D.A.; Moreno, F.B.; Monteiro-Moreira, A.C.O.; Alencar, L.M.R.; Abreu, A.S.G.; Sousa, J.S.; Oliveira, J.T.A. A 2S Albumin from the Seed Cake of Ricinus Communis Inhibits Trypsin and Has Strong Antibacterial Activity against Human Pathogenic Bacteria. *J. Nat. Prod.* **2016**, *79*, doi:10.1021/acs.jnatprod.5b01096.